Received: 9 June 2025 | Accepted: 13 May 2026

DOI: 10.1111/1365-2435.70374

Functional Ecology

RESEARCH ARTICLE

# Linking rhizosphere bacterial succession to metabolite dynamics unravels the underlying survival strategies of desert ephemeral plants

Yang Yang[1,2] | Weiguo Liu[1,2] | Xi-En Long[3] | Yangyang Jia[1,2] | Xiaodong Yang[1,4]

[1]College of Ecology and Environment, Xinjiang University, Urumqi, China

[2]Key Laboratory of Oasis Ecology of Education Ministry, Urumqi, China

[3]School of Geographic Sciences, Nantong University, Nantong, China

[4]Department of Geography and Spatial Information Technology, Ningbo University, Ningbo, China

**Correspondence**
Weiguo Liu
Email: wgliuxj@xju.edu.cn

Xiaodong Yang
Email: xjyangxd@sina.com

**Funding information**
Key Laboratory Project, Xinjiang, Grant/Award Number: 2021D0400; National Natural Science Foundation of China, Grant/Award Number: 32160281 and 32460321

**Handling Editor:** Katie Jayne Field

## Abstract

1. Desert ephemerals complete rapid life cycles to survive aridity, yet the ontogenetic coordination of below-ground rhizosphere interactions with above-ground resource allocation remains unclear.
2. This study examined six dominant ephemeral species (*Eremurus inderiensis*, *Eremopyrum orientale*, *Erodium oxyrrhynchum*, *Allium mongolicum*, *Alyssum linifolium* and *Nepeta micrantha*) in the Gurbantünggüt Desert across seedling and flowering stages, integrating plant biomass, rhizosphere metabolites and bacterial communities.
3. This study detected consistent ontogenetic shifts at the overall level: a 44.4% decrease in root: shoot ratio shifting biomass from below-ground to above-ground with interspecific variations. Concurrently, rhizosphere metabolic space contracted by 86.4%, with species-specific metabolic plasticity strongly correlated with biomass reallocation magnitude. Bacterial communities exhibited reduced α-diversity, simplified co-occurrence networks and a predicted functional transition from carbon to nitrogen metabolism. Keystone microbe–metabolite associations shifted from carbon-based linkages at the seedling stage to nitrogen-centric correlations at flowering, accompanied by stage-specific turnover of keystone taxa and reconfiguration of microbe–metabolite networks. At the species level, however, the key taxa, metabolites and network dynamics underlying these shifts were highly specific, with divergent niche-width dynamics and stage-specific interactions corresponding to host metabolic plasticity. Path modelling revealed a universal, stage-dependent reversal in biomass drivers: below-ground biomass was initially supported by broad bacterial niche width, whereas flowering-stage above-ground biomass was directly driven by rhizosphere metabolites.
4. These findings demonstrate that host developmental stage orchestrates a phased rhizosphere strategy in desert ephemerals. This strategy synchronizes keystone taxa succession and microbe–metabolite network reconfiguration with plant ontogenetic goals, enabling a conserved shift from microbial-assisted

Weiguo Liu and Xiaodong Yang contributed equally to this work.

This is an open access article under the terms of the Creative Commons Attribution License, which permits use, distribution and reproduction in any medium, provided the original work is properly cited.
© 2026 The Author(s). *Functional Ecology* published by John Wiley & Sons Ltd on behalf of British Ecological Society.

establishment to metabolite-driven reproduction despite species-specific pathways. This study provides novel insights for plant–microbe co-adaptation in resource-limited desert ecosystems.

**KEYWORDS**
ephemeral plants, microbe–metabolite association network, niche width, plant biomass, rhizosphere bacterial community

## 1 | INTRODUCTION

Global climate change and intensifying droughts threaten desert ecosystem productivity (Neilson et al., 2012). Desert ephemerals, key components, avoid drought by completing life cycles during brief wet seasons (Fan et al., 2022). This strategy, synchronized with snowmelt and spring rains, allows biomass accumulation and secures their role in primary production and nutrient cycling (Huang et al., 2015; Zeng et al., 2016). The success of this functional group is hypothesized to rely on precise developmental programming and efficient root-shoot resource allocation (Nour et al., 2024). However, the internal mechanisms governing these transitions remain poorly understood, particularly how plant–rhizosphere interactions coordinate below- and above-ground investments.

In the rhizosphere, plant roots shape microbial communities through metabolite exudation, serving dual roles as nutrients and chemical signals to recruit beneficial microorganisms (Hemelda & Noutoshi, 2025). In nutrient-poor desert ecosystems, this interaction is crucial for nutrient cycling. For instance, Gemmatimonadetes and Bacteroidetes re-release nitrogen and phosphorus by decomposing senesced plants, thereby synchronizing microbial activity with plant phenology to maximize resource-use efficiency (Araya et al., 2019; Zhang et al., 2020). This below-ground assembly is primarily driven by plant developmental stage (Fan et al., 2025), as shifting physiological priorities shape rhizosphere 'microbial fingerprint' changes (Zhalnina et al., 2018). For example, root exudates in early growth recruit decomposers to meet high nutrient demands, while in later reproduction, exudate composition shifts to redeploy resources and induce adaptive microbial changes (Lei et al., 2025). These stage-dependent shifts are reflected in microbial diversity (Yang et al., 2025), niche width (Jiang et al., 2023) and interaction networks (Fan et al., 2025). However, for desert ephemerals, patterns of these developmental changes and their ecological consequences remain insufficiently understood. A key limitation of current research is focusing mainly on single time points rather than dynamic processes, leaving a critical knowledge gap in dynamic mechanisms across the full growth cycle.

The Gurbantünggüt Desert, China's most extensive fixed and semi-fixed dune desert, sustains widespread ephemeral plants (Fan et al., 2022). To test the hypothesis that developmental stage transitions drive coordinated shifts in plant biomass allocation, rhizosphere metabolite profiles and bacterial community assembly, this study investigated dominant ephemeral plant species in this system. We aimed to elucidate: (1) how biomass reallocation patterns and rhizosphere metabolite profiles are restructured during the transition from seedling to flowering stages; (2) how rhizosphere bacterial diversity, niche width and co-occurrence networks respond to plant development; (3) how rhizobacteria-metabolite associations change over time; and (4) how these interconnected dynamics ultimately feedback to influence plant biomass accumulation. This study seeks to reveal the ecological mechanisms through which ephemeral plants optimize performance in extreme environments.

## 2 | MATERIALS AND METHODS

### 2.1 | Study site

This study was conducted at the southern margin of the Gurbantünggüt Desert in Xinjiang, China (Figure 1). The region has a temperate continental arid climate: mean annual precipitation of 100–150 mm (over 65% from snowmelt and spring rains), mean annual evaporation >2000 mm and a mean annual temperature of 5–7°C (Zhao et al., 2023). In spring, the total vegetation coverage is approximately 15%–50% (Li et al., 2021). Among this vegetation, annual plants account for around 50% of the total vegetation coverage (Chen et al., 2008). We focused on six dominant ephemeral species: *Eremurus inderiensis* (D), *Eremopyrum orientale* (DF), *Erodium oxyrrhynchum* (MN), *Allium mongolicum* (SC), *Alyssum linifolium* (TY) and *Nepeta micrantha* (XH). These species are widely distributed on dunes and are the dominant species in the local area (Chen et al., 2019; Fan et al., 2022). Detailed species information is available in Supporting Information (Figures S1–S3; Tables S1 and S2).

No official permits or licences were required for all field sampling and field investigations in the present study. All field work complied with local relevant research regulations.

### 2.2 | Sample collection

Sampling covered two phenological stages. The seedling stage was characterized by three to four fully expanded true leaves and no reproductive organs (sampled on 8 April 2024). The flowering stage occurred when over 80% of adult individuals of the target ephemeral species bloomed synchronously, forming large, contiguous flower clusters on the soil surface (sampled on 5 May 2024). Sampling

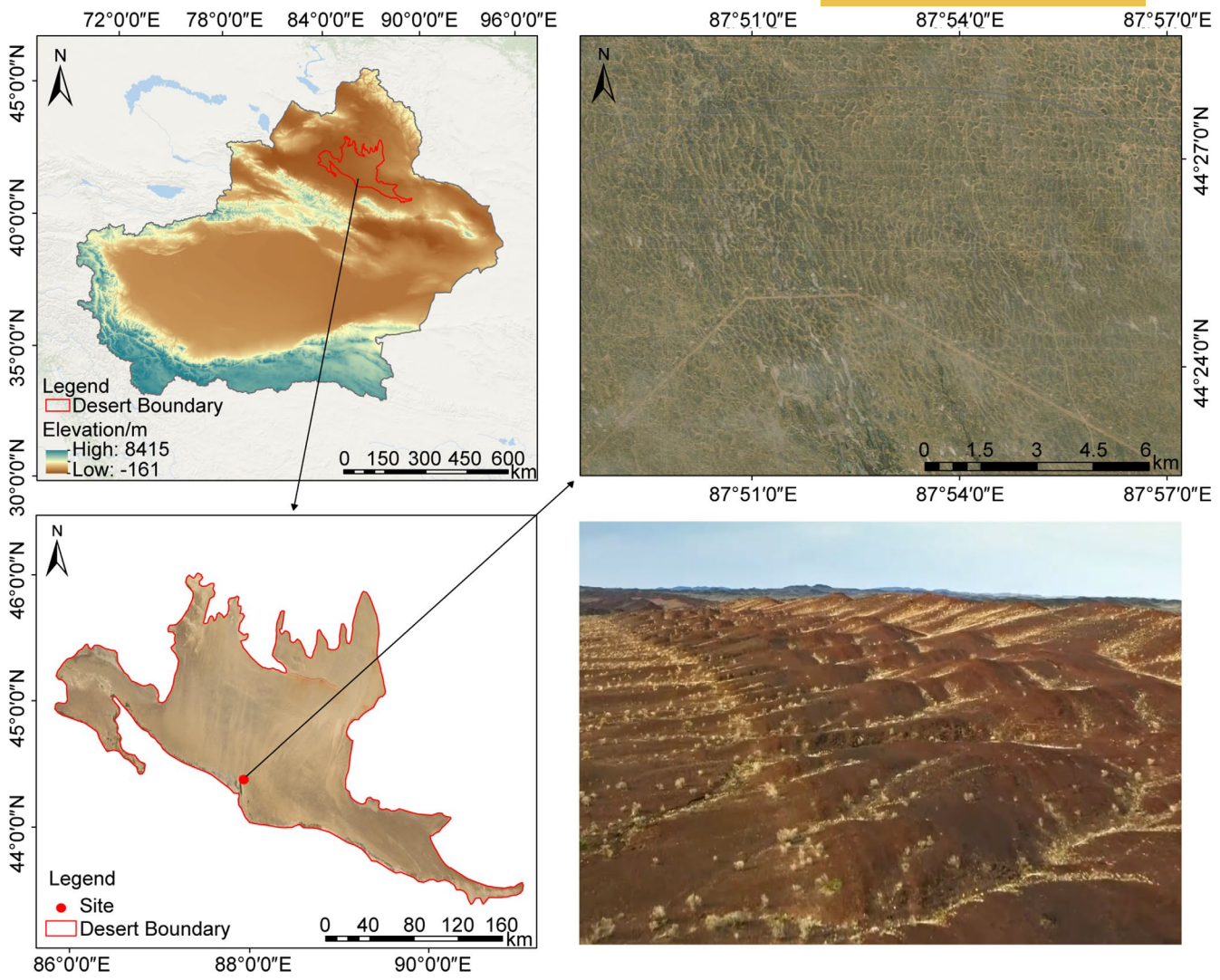



FIGURE 1 Location and landscape of the study area.

TABLE 1 Replication statement.

| Scale of inference | Scale at which the factor of interest is applied | Number of replicates | | | |
|---|---|---|---|---|---|
| | | Species | Dune | Stage | Total |
| Rhizosphere bacteria | Individual | 6 | 6 | 2 | 72 |
| Rhizosphere metabolites | Individual | 6 | 6 | 2 | 72 |
| Soil properties | Individual | 6 | 6 | 2 | 72 |

was conducted at 6 randomly selected independent sand dunes (inter-dune distance ≥1 km; Edwards et al., 2015). On each dune, 20–25 healthy individuals per species were randomly selected (≥2 m between any two conspecific individuals). The entire root system of each plant was excavated. After removing loose soil, we collected the rhizosphere soil (tightly adhering to roots) using a sterile soft-bristled brush (Edwards et al., 2015). Rhizosphere soils from all selected individuals of the same species per dune were pooled into one composite sample. During each growth stage, one independent composite sample was obtained per dune for each species, resulting in a total of 36 samples across the six plant species. Upon collection, all soil samples were immediately placed in either liquid nitrogen or dry ice and promptly transported to the laboratory. Samples were subdivided into three aliquots (Table 1): two for DNA extraction and soil metabolomic analysis (stored at −80°C), and one for soil physicochemical analysis (stored at 4°C). Soil properties, including soil water content (SWC), pH, electrical conductivity (EC), soil organic carbon (SOC), total nitrogen (TN), available phosphorus (AP) and available potassium (AK), were determined using standard methods (Bao, 2000).

Plant biomass was sampled concurrently. Above-ground biomass (AGB) and below-ground biomass (BGB) were separated using sterile

scissors. Roots were rinsed with deionized water to remove soil and blotted dry with sterile filter paper. All samples were placed in pre-weighed paper bags, oven-dried at 75°C (≥48 h) to constant weight and weighed to determine dry mass.

### 2.3 | DNA extraction and sequencing

Genomic DNA was extracted from 0.25 g of homogenized soil using the CTAB method. 16S rRNA gene V4 region was amplified (515F/806R) and sequenced on Illumina NovaSeq 6000 (Caporaso et al., 2011; Kozich et al., 2013). Raw reads were demultiplexed, quality-filtered and merged to obtain high-quality sequences. Amplicon Sequence Variants (ASVs) were inferred and taxonomically classified against the SILVA 138.1 database (Quast et al., 2013). After rarefying to an even sampling depth, the ecological functions of the bacterial community were predicted using FAPROTAX (Louca et al., 2016).

### 2.4 | Metabolomics analysis

Approximately 50 mg of soil from each composite sample was used for metabolite extraction. Metabolites were extracted with 500 μL of a pre-cooled (−20°C) 70% methanol solution containing internal standards and 300 μL of dichloromethane and then vortexed mixing for 3 min. After centrifugation at 12,000 rpm for 10 min at 4°C, 300 μL of the supernatant was transferred to a new 1.5-mL tube and incubated at −20°C for 30 min. Centrifugation was repeated, and 200 μL of the resulting supernatant was processed through a protein precipitation plate for online analysis. All extracts were stored at −20°C until further use. Metabolite profiling was performed using an ultra-performance liquid chromatography (UPLC) system coupled to a QTRAP® 6500+ tandem mass spectrometer. Each sample had three technical replicates to reduce instrumental errors, with mean ± SD as final data for analysis. Metabolites were identified by matching acquired mass spectra to the KEGG Compound database. A permutation test (200 permutations) was applied to evaluate model robustness.

### 2.5 | Statistical analysis

All analyses were conducted in R v4.3.3. Biomass allocation patterns were assessed using *t*-tests, with effect sizes calculated via Cliff's delta. Metabolomic profiles were analysed using principal component analysis (PCA). PERMANOVA (999 permutations) with a full factorial model tested effects of species, developmental stage and their interaction at the overall level. Metabolic plasticity was quantified as Euclidean distance in PCA space between developmental stages per species. Differential metabolites were identified with $|\log_2 FC| > 0.5$, Wilcoxon rank-sum tests ($p < 0.05$) and ≥67% species consistency for conserved patterns. Pearson correlation assessed relationships between metabolic plasticity and biomass allocation (overall-level only). Dispersion homogeneity was verified using PERMDISP (overall-level only).

Rhizosphere bacterial α-diversity (Shannon, Simpson, Pielou, Chao1) and niche width (Levin's B metric) were compared via *t*-tests, with generalists/specialists identified accordingly (Wilson & Hayek, 2015). PERMANOVA quantified effects on bacterial community structure. Rhizobacterial composition differences were determined using STAMP, and community structure was visualized by principal coordinates analysis (PCoA) based on Bray–Curtis distance. For FAPROTAX-predicted functional composition, PERMANOVA quantified effects of compartment and growth stage at overall level only. Functional profiles were preprocessed by removing functions with mean abundance <0.01% and irrelevant categories (Knight et al., 2018; Wen et al., 2023) before PCoA (Jaccard distance).

Environmental variable contributions were quantified via Redundancy Analysis (RDA). Co-occurrence networks were constructed from bacterial genera (relative abundance >0.005 in ≥50% of samples) based on Spearman correlation ($|r| > 0.7$, $p < 0.05$; Wang et al., 2023). Keystone taxa were identified using *Zi-Pi* thresholds (Olesen et al., 2007). For functional comparisons, non-parametric Wilcoxon signed-rank tests were used at the overall level; species-level comparisons employed paired *t*-tests or Wilcoxon signed-rank tests based on normality (Liu, Mansoldo, et al., 2025). Predicted functional contributions were assessed via PLS regression (VIP > 1) and correlations. Associations between key taxa and metabolites were assessed using Spearman correlation ($|r| > 0.6$, $p < 0.05$) and visualized in hierarchical clustering heatmaps. Relationships between bacterial niche width and plant biomass were examined via ordinary least squares (OLS) regression (overall-level only). Partial least squares path modelling (PLS-PM) evaluated integrated effects of soil metabolites, niche width, α-diversity and keystone taxa on AGB and BGB (overall-level only).

## 3 | RESULTS

### 3.1 | Plant growth dynamics and rhizosphere environment

Biomass allocation underwent significant below-ground-to-above-ground shifts across all six species during development (Figure 2a, Figure S4, $p < 0.05$), with overall root: shoot ratios decreasing by 44.4% (Welch's *t*-test: $p = 4.5 \times 10^{-8}$). Shift magnitude differed markedly, ranging from dramatic (DF: 45.20%, SC: 44.30%) to conservative (XH: 3.36%) (Table S3).

The soil had a substantial decline in SWC ($p < 0.05$); soil nutrients decreased but EC increased ($p < 0.05$, Figure S5). Rhizosphere soil metabolites comprised eight categories at seedling and seven at flowering stages, with amino acids consistently dominant (Figure 2b). PCA revealed profound restructuring of rhizosphere metabolites ($R^2 = 0.085$, $p = 0.001$), characterized by an 86.4% metabolic

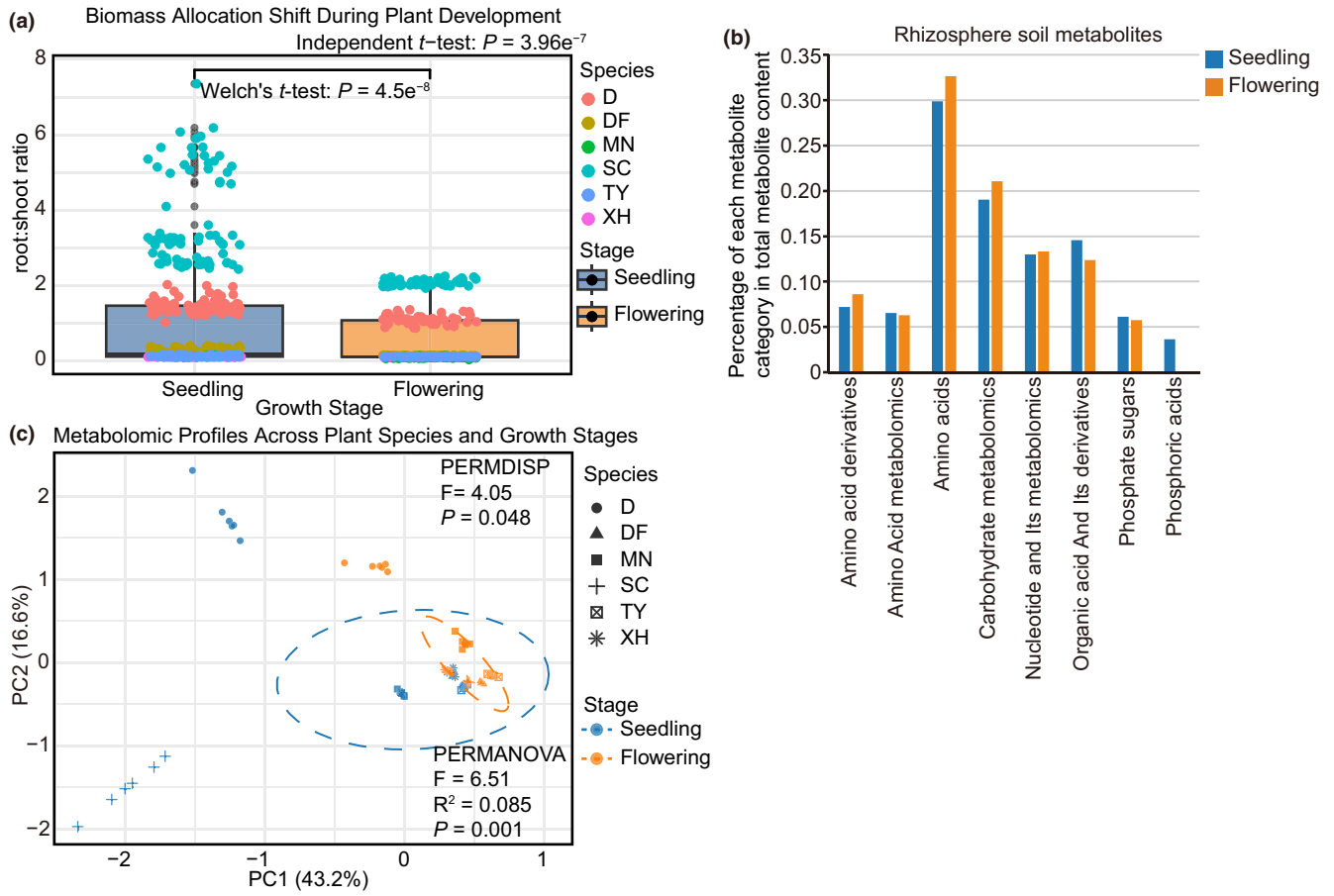



FIGURE 2 (a) Biomass allocation patterns across desert ephemeral species and growth stages. (b) Proportions of rhizosphere metabolite categories across species and growth stages. (c) Developmental restructuring of rhizosphere metabolomic profiles.

space contraction from seedling to flowering (Figure 2c; Table S4). PERMANOVA showed plant species identity as the primary driver of metabolic variation ($R^2 = 0.508$, $p < 0.001$), followed by a highly significant species × stage interaction ($R^2 = 0.399$, $p < 0.001$), while developmental stage alone explained 0.085 of variance (Table S5). Species exhibited marked metabolic plasticity during the seedling-to-flowering transition (Table S6): SC had the highest (2.744), followed by D (1.236) and MN (0.754), while DF (0.225), TY (0.247) and XH (0.031) had minimal. Notably, metabolic plasticity strongly negatively correlated with root: shoot ratio changes across species ($r = -0.958$, $p = 0.0025$; Figure S6ce).

Pronounced flowering-stage metabolic specialization reflected species-specific adaptations and conserved developmental patterns (Figure S7, Tables S7 and S8). Distinct species-specific signatures emerged: D accumulated L-citrulline, Ornithine and DL-Glyceric-Acid while depleting Glutamine and L-Asparagine; DF and XH elevated Ornithine while down-regulating L-Glutamic-acid, Glutamine and Trehalose-6-phosphate; SC suppressed multiple amino acids (L-Asparagine, L-Leucine and Serine); MN and TY enhanced L-leucine and DL-Glyceric-Acid. Beyond these species-specific patterns, four conserved metabolites that were consistently significantly altered ($|\mathrm{Log_2FC}| > 0.5$, $p < 0.05$ in at least four species): AMP, Gluconate, Glutamine and L-Glutamic-acid.

## 3.2 | Taxonomy, niche width and diversity dynamics of rhizobacterial community

A total of 24,339 and 7248 bacterial ASVs were detected at the seedling and flowering stages, respectively, with rarefaction curves confirming adequate sampling depth (Figure S8). Multivariate analyses indicated that the rhizobacterial community was shaped collectively by plant species, growth stage and environmental factors, together explaining 77.9% of variation ($p = 0.001$, Figure 3a). RDA identified plant species as the strongest determinant ($R^2 = 0.188$), followed by growth stage ($R^2 = 0.122$) and soil nutrients (Figure 3b; Table S9). At the species level, developmental stage consistently structured rhizobacterial communities. All six species showed significant compositional shifts between seedling and flowering stages (PERMANOVA, $p < 0.05$; RDA, $p < 0.01$; Figure S9a), whereas soil factors had no significant effect within any species (Table S10). Beta-diversity analysis further supported the dominant role of growth stage, with between-stage distances (0.426–0.512) exceeding within-stage distances across all species (seedling: 0.111–0.238; flowering: 0.122–0.171).

The overall and species-specific rhizobacterial α-diversity (Shannon, Simpson and Pielou) showed a consistent decrease. However, overall Chao1 richness increased, with non-significant

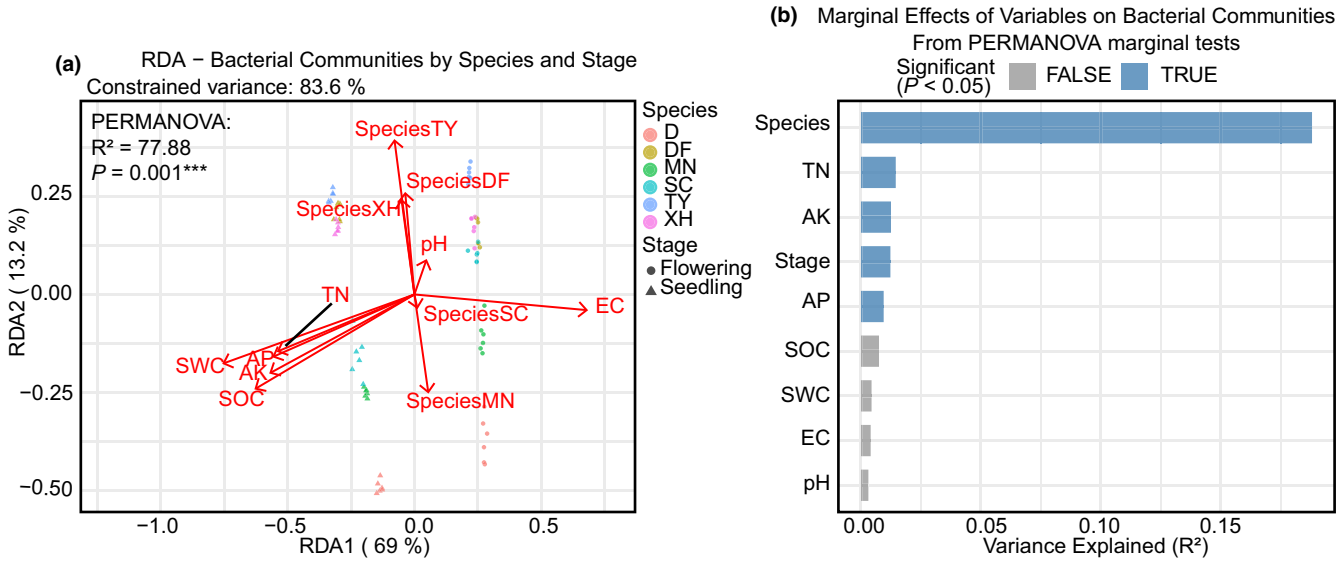



**FIGURE 3** Overall Redundancy Analysis (RDA) and marginal effects of explanatory variables on rhizobacterial communities of desert ephemeral plants. (a): RDA with environmental vectors. (b) Independent contributions (marginal $R^2$, 999 permutations) of each factor.

reductions only in TY and XH (Figure 4a, Figure S10). Niche width remained stable overall but diverged among species: it expanded significantly in TY and XH but contracted in D and SC (Figure 4b, Figure S11a). Concurrently, the specialist-to-generalist ratio was reconfigured from seedling to flowering stages (Figure 4c, Table S11). D and SC increased specialist proportions, whereas others reduced them (Figure S11b, Table S12). Bacterial communities differed significantly between rhizosphere and bulk soil ($R^2$=0.166, $p$=0.001). Within the rhizosphere, developmental stage was the dominant driver of community structure ($R^2$=0.453, $p$=0.001; Figure 4d). Within each developmental stage, bacterial community structure differed markedly among species (seedling: $R^2$=0.897, $p$=0.001; flowering: $R^2$=0.859, $p$=0.001; Figure S11c).

STAMP analysis revealed that the enrichment patterns of rhizosphere soil bacteria at the phylum level differed from those of bulk soil during the seedling and flowering stages (Figure S12). Within the rhizosphere, Actinobacteria and Proteobacteria dominated both stages, with Proteobacteria increasing (27.6% to 29.9%) while Firmicutes (5.3% to 3.9%) and Gemmatimonadota (3.7% to 2.1%) declined significantly (Figure 4e). Changes in specific phyla varied among species (Figure S13–S15).

FAPROTAX-predicted functional composition differed significantly between rhizosphere and bulk soil ($R^2$=0.128, $p$=0.001), with developmental stage as the primary driver of rhizobacterial functional divergence ($R^2$=0.370, $p$=0.001; Figure 5a). With plant growth, the overall rhizosbacterial FAPROTAX-functional profile shifted systematically: carbon cycle-related functions were suppressed, while nitrogen cycle-related functions were enhanced (Figure 5b). Chemoheterotrophy, cellulolysis and fermentation were down-regulated, whereas nitrogen_fixation, nitrate_reduction and nitrite_ammonification were significantly up-regulated, alongside a marked increase in arsenate_detoxification (Figure 5c). This functional shift was conserved across five species (DF, MN, SC, TY and XH). In contrast, D exhibited the opposite pattern: flowering-stage rhizosphere exhibited enhanced complex carbon degradation (e.g. xylanolysis and cellulolysis), while nitrogen cycling pathways (e.g. nitrate_reduction) showed no significant induction and a non-significant decrease (Figure S16, Table S13).

### 3.3 | Dynamics of rhizobacterial co-occurrence networks

Rhizosphere networks were markedly more complex than those in bulk soil. Overall rhizobacterial co-occurrence networks underwent significant structural simplification from seedling to flowering stages, reflected in reduced node/edge counts (213 to 141; 1538 to 708), lower average degree (14.44 to 10.04), increased positive interactions (70.35% to 81.21%) and decreased modularity (Figure 6, Table S14). Most species followed this trend except SC and MN, which showed increased complexity (Figure S16, Table S15). Species diverged in network strategies: D and DF exhibited clear simplification; SC and MN enhanced connectivity (average degree: 4.20, 2.66 to 7.05, 3.70, respectively), while TY and XH improved integration through shortened average path length.

In the overall co-occurrence network, keystone taxa identified via *Zi-Pi* analysis exhibited striking stage-specific functional contributions (Figures 6a and 7a; VIP >1). Seedling core taxa comprised *Roseomonas*, *Arthrobacter*, *Duganella* and *Pontibacter*, while flowering stages were dominated by *Blastocatella*, *Truepera* and *Rhodopirellula*.

Predicted functional contributions of species-specific key genera also showed strong host and stage specificity (Figure 7b, Figures S18 and S19). Core taxa displayed minimal inter-/intra-specific overlap across stages, with no congruence with overall network core genera (Table S16). For instance, D harboured *Lachnospiraceae_NK4A136_group* and *Geodermatophilus* at the

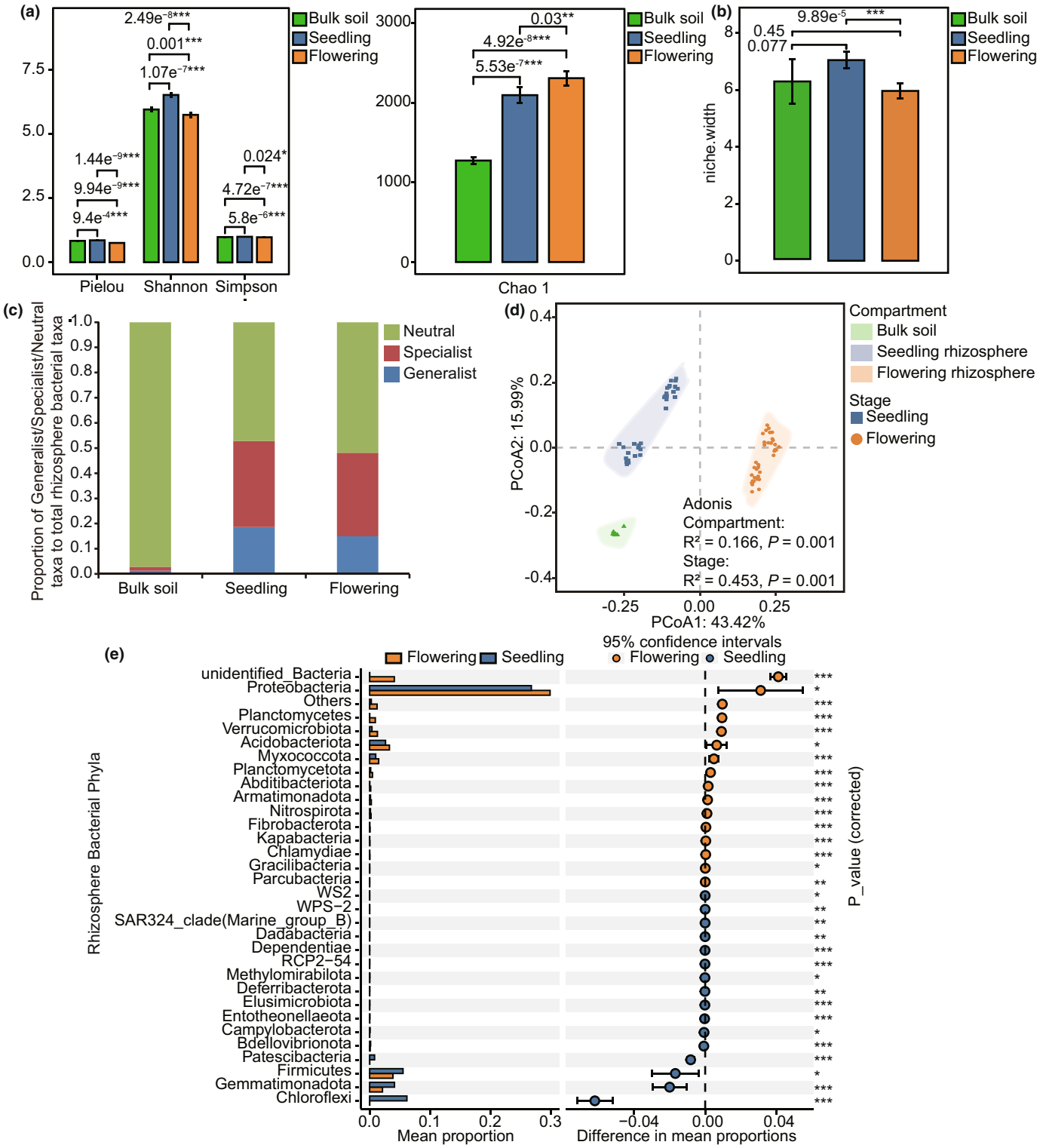



FIGURE 4 Comparisons of bacterial communities in rhizosphere and bulk soil. (a, b) Bacterial α-diversity and niche width across bulk soil, seedling and flowering rhizosphere. ***$p < 0.001$, **$p < 0.01$, *$p < 0.05$. (c) Proportions of generalist, specialist and neutral taxa in bulk soil, seedling and flowering rhizosphere. (d) Principal coordinates analysis (PCoA) of bacterial community structure. (e) Differentially abundant rhizobacterial phyla between two growth stages. ***$p < 0.001$, **$p < 0.01$, *$p < 0.05$.

seedling stage, replaced by *Negativibacillus* and *unclassified_Oligoflexia* at flowering. SC was dominated by *Edaphobaculum* at the seedling stage, while *Nocardioides* and *Pseudorhodoplanes* prevailed at flowering. All other species also possessed unique stage-specific high-contribution taxa.

### 3.4 | Linkages between metabolites and key bacterial taxa

The proportion of significant microbe–metabolite associations decreased from 54.3% at seedling to 30.0% at flowering (Figure 8a).

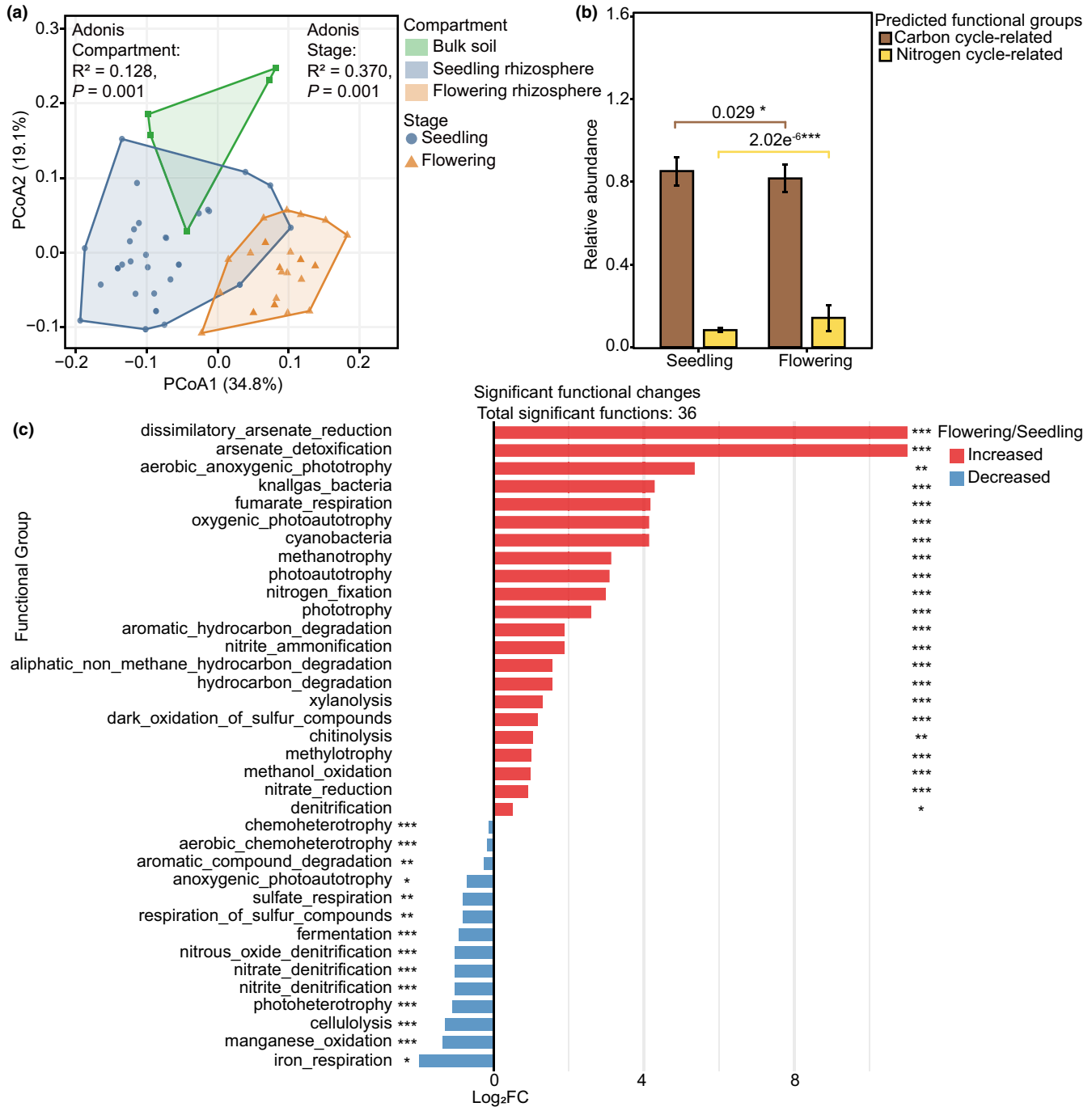



**FIGURE 5** Dynamic changes in FAPROTAX-predicted functional potentials of rhizobacterial communities across plant growth stages. (a) Principal coordinates analysis (PCoA) of FAPROTAX-functional composition. (b) Dynamics of predicted carbon- and nitrogen-related functional groups during plant growth. ***$p < 0.001$, **$p < 0.01$, *$p < 0.05$. (c) Predicted functions with significant changes at the overall level. Bar charts show the $Log_2FC$ of microbial functions (Flowering vs. Seedling). Red bars: $Log_2FC > 0$ (up-regulated at flowering); blue bars: $Log_2FC < 0$ (down-regulated at flowering). ***$p < 0.001$, **$p < 0.01$, *$p < 0.05$ (FDR-corrected).

Networks contracted in D, DF and XH but expanded markedly in SC and TY, while MN remained stable across stages. During the seedling stage, seven keystone microorganisms correlated strongly ($|r| > 0.6$, $p < 0.05$) with 12 metabolites (Figure 8b,c). Among them, *Arthrobacter* and *Duganella* correlated positively with carbon metabolites, such as DL-Glyceric-Acid and Trehalose-6-phosphate, whereas *Roseomonas*, *Roseisolibacter* and *Sumerlaea* showed negative correlations with the same compounds. At flowering, six keystone microorganisms correlated with eight metabolites (Figure 8d,e). *Blastocatella*, *Rhodopirellula* and *Truepera* correlated negatively with L-Aspartate and Trehalose-6-phosphate, while *Microbacterium* and *unidentified_Rhizobiales* correlated positively with Glutamine and L-Glutamic-acid but negatively with Cysteic-acid.

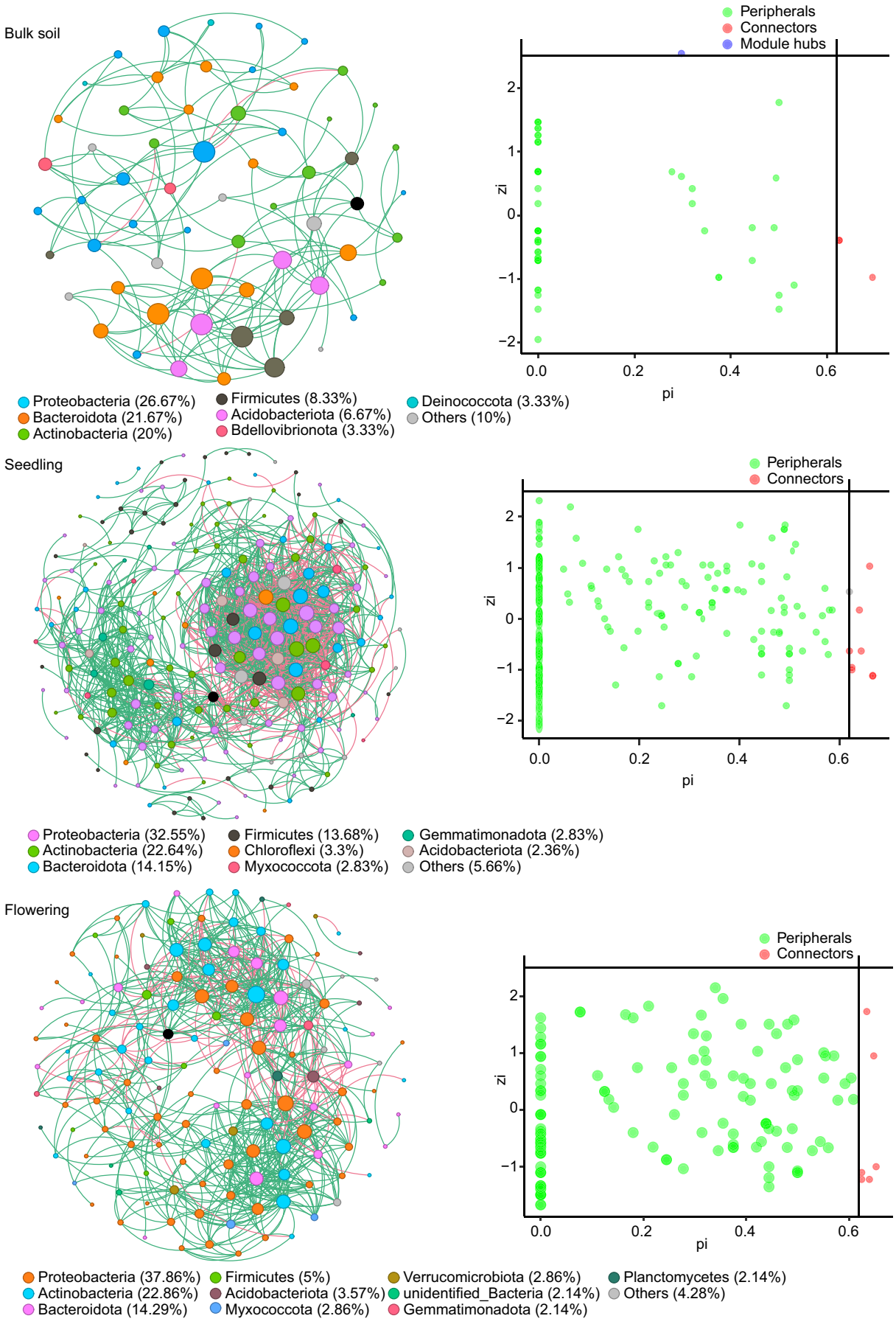



**FIGURE 6** Co-occurrence network of soil bacteria in bulk soil and rhizosphere across plant growth stages. Green and red arrows indicate positive and negative effects, respectively. Nodes represent bacterial genera, sized by average degree. The *Zi-Pi* plot highlights the roles of genera of bacterial community based on topological properties.

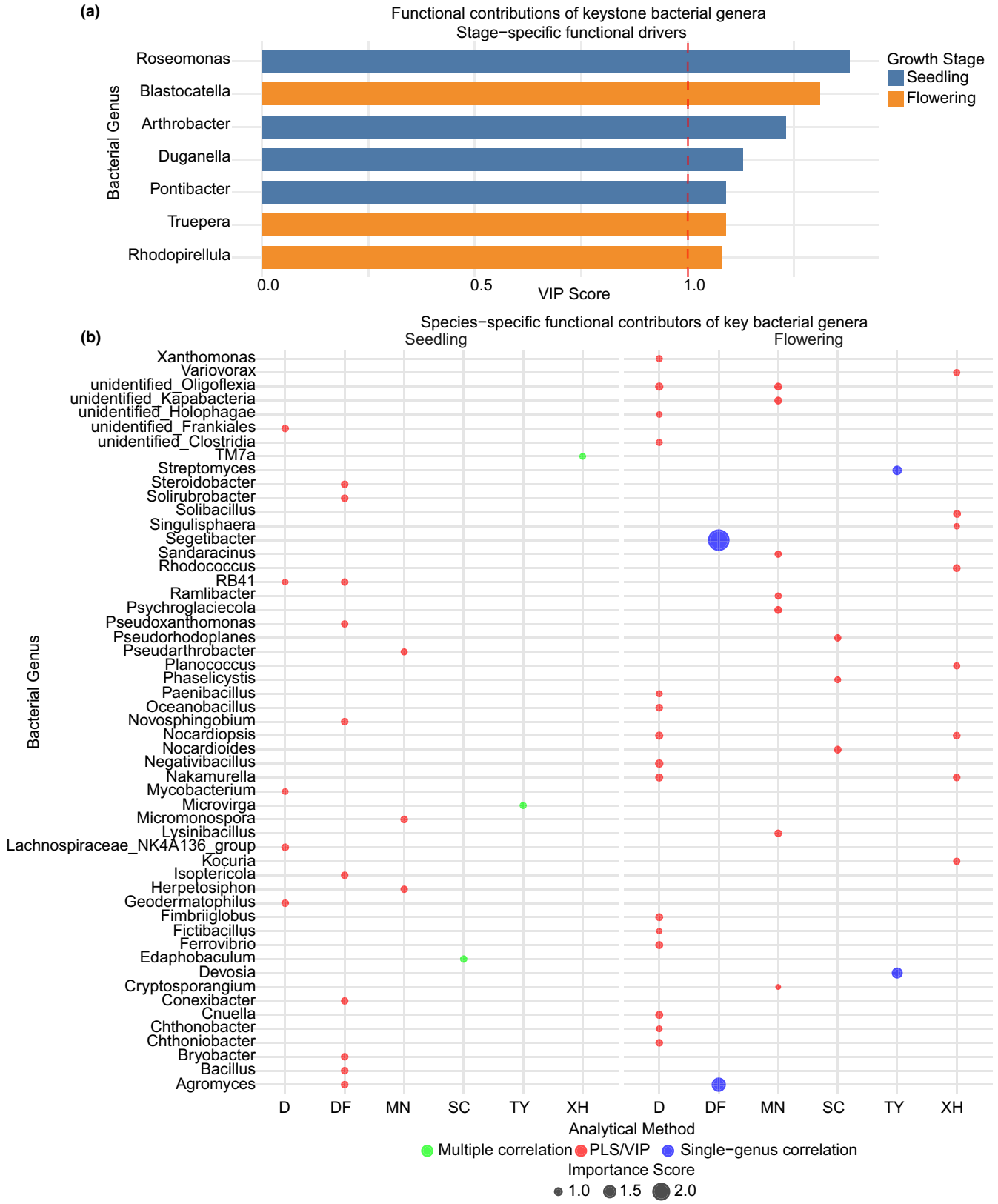



FIGURE 7 FAPROTAX-functional contributions of keystone bacterial genera. (a) Stage-specific functional drivers. The bar chart sorts the genera by VIP value. (b) Species-specific functional contributors of key bacterial genera. Bubble size indicates the importance score of the bacterial genus. Colours indicate analytical methods: Green (multiple correlation), red (PLS/VIP) and blue (single-genus correlation).

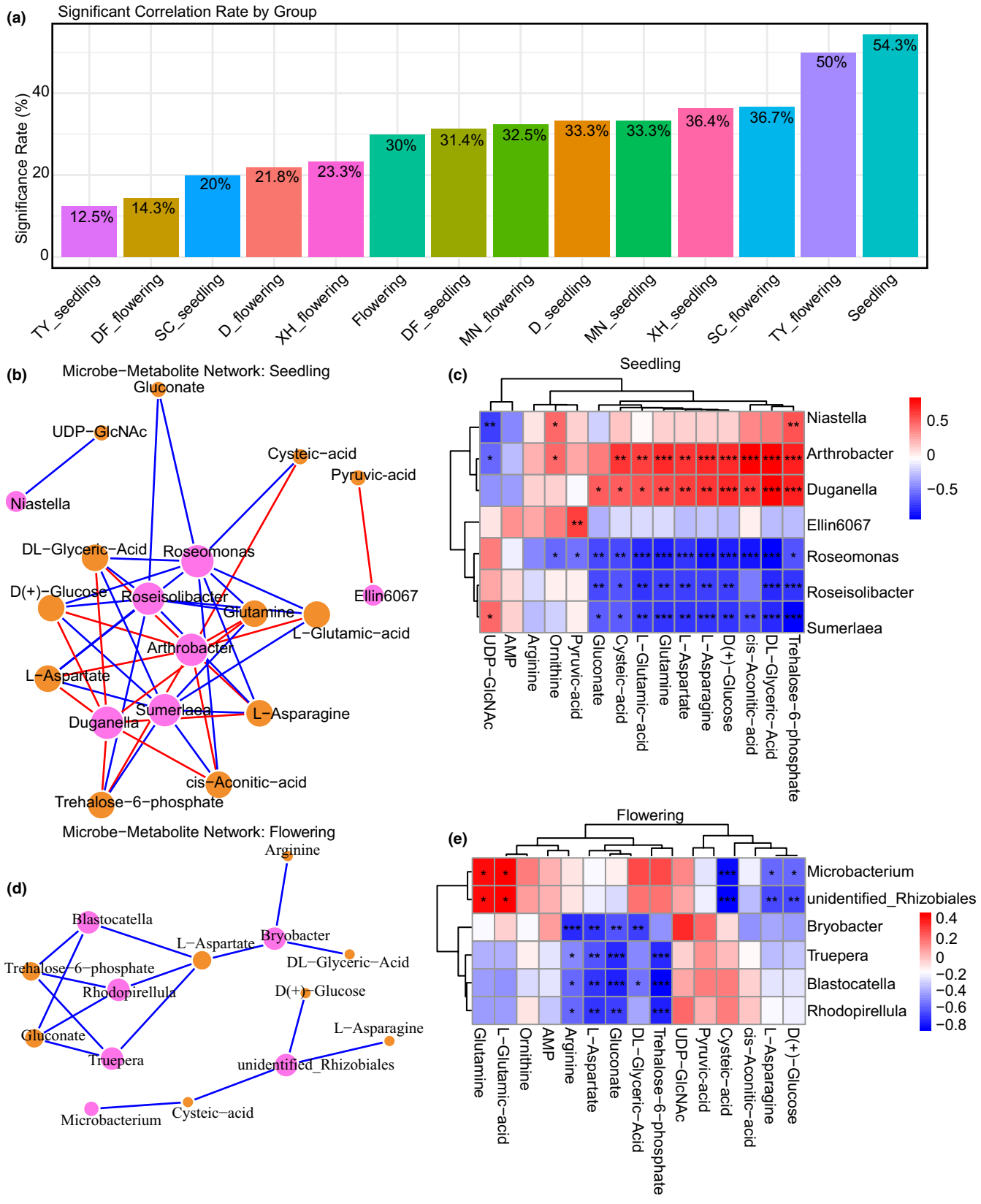



**FIGURE 8** Microbe–metabolite associations across stages. (a) Significant association ratio of each species across stages. (b, c) Overall keystone taxa–metabolite association networks at seedling/flowering stages. Red and blue arrows indicate positive and negative effects, respectively. Pink and orange nodes indicate keystone taxa and metabolites, sized by average degree, respectively. (d, e) Correlation heatmaps of overall keystone taxa–metabolite associations at seedling/flowering stages. Colour gradient indicates Pearson correlation coefficient (*r*). ***$p < 0.001$, **$p < 0.01$, *$p < 0.05$.

Species-specific analyses uncovered distinct stage-dependent linkage patterns (Figures S20–S22). In D, *RB41* and *unidentified_Frankiales* correlated positively with L-Aspartate, L-Glutamic-acid and AMP at the seedling stage. By flowering, *Ferrovibrio* and *unidentified_Oligoflexia* associated positively with L-Aspartate and Gluconate. DF transitioned from nine bacterial taxa associated with Ornithine to only *Agromyces* and *Segetibacter* correlating with L-Glutamic-acid. MN and TY had consistent microbial–metabolite dynamics, with keystone microbes showing opposing correlations with the same metabolites across stages. In SC, *Edaphobaculum* correlated negatively with AMP and positively with Pyruvic-acid and Trehalose-6-phosphate at the seedling stage. At flowering, *Nocardioides* and *Pseudorhodoplanes* were positively linked to L-Aspartate, Ornithine and Pyruvic-acid, but negatively linked to Glutamine. In XH, *TM7a* was positively correlated with Glutamine and Trehalose-6-phosphate but negatively correlated with AMP and Pyruvic-acid at the seedling stage. At flowering, *Nakamurella* were positively correlated with Arginine and L-Glutamic-acid and negatively correlated with cis-Aconitic-acid.

### 3.5 | Stage-dependent reversal in microbial and metabolite regulation of plant biomass

OLS showed significant positive correlations between bacterial niche width and both AGB ($R^2=0.19$, $p<0.05$) and BGB ($R^2=0.30$, $p<0.05$; Figure 9a). PLS-PM explained high proportions of variance in AGB (80.1%) and BGB (85.1%) at seedling stage, decreasing to 69.8% and 65.6%, respectively, at flowering (Figure 9b,c). Path analysis uncovered a clear stage-dependent reversal in ecological effects. At the seedling stage, both bacterial niche width (AGB: 2.2939; BGB: 1.8926) and keystone taxa (AGB: 0.5788; BGB: 0.9417) significantly promoted biomass accumulation. In contrast, soil metabolites exhibited negative direct effects on biomass (AGB: −1.2215; BGB: −0.065). This pattern reversed completely at the flowering stage. Bacterial niche width (AGB: −0.4822; BGB: −0.6962) and keystone taxa showed negative effects on biomass. Meanwhile, soil metabolites exerted strong positive direct effects on both AGB (0.7318) and BGB (1.0925). Furthermore, bacterial α-diversity negatively affected niche width at the seedling stage (−0.5574), a relationship that weakened to non-significant at flowering. Concurrently, diversity demonstrated a significant negative impact on AGB (−0.4388) during the flowering stage.

## 4 | DISCUSSION

### 4.1 | Dynamic biomass allocation, metabolic restructuring and divergent ecological strategies

This study revealed pronounced BGB to AGB reallocation as desert ephemerals transitioned from seedling to flowering stages (Figure 2a, Figure S4). The sharp root: shoot ratio reduction highlighted a resource-priority shift under resource-limited desert conditions (Ding et al., 2025) and represented a key signature of the drought-escape strategy (Poorter et al., 2012). Interspecific differences in biomass allocation were associated with lineage-specific adaptive traits, reflecting long-term evolutionary adaptation to the Gurbantünggüt Desert. D relies on a lineage-specific fleshy taproot for resource storage at the seedling stage, whereas MN coordinates water uptake and soil exploration via succulent leaves and a shallow, spreading root system. Their moderate biomass redistribution reflected a classic below-ground establishment–above-ground reproduction trade-off (Poorter et al., 2012). As accelerated allocation strategists, DF rapidly constructs above-ground photosynthetic structures via tillering, while SC mobilizes pre-stored bulb reserves for reproduction. Both complete seed production before severe drought, aligning with global stress-driven resource allocation (Peng et al., 2022). By contrast, TY and XH exhibited a conservative strategy, maintaining greater below-ground investment to exploit late-season moisture pulses (Funk et al., 2024; Puglielli et al., 2021).

Biomass reallocation coincided with extensive rhizosphere metabolome restructuring. While developmental stage drove metabolite remodelling, plant species identity and its stage interaction explained most metabolic variation (Figure 2c, Table S5). Metabolic niche contraction signalled a shift from exploratory to specialized rhizosphere chemical interactions (Hacquard & Martin, 2024), mediated by host genotype (Pacheco-Moreno et al., 2024). These lineage-specific shifts reflect adaptive differentiation under resource limitation in the desert (She et al., 2017). High-plasticity species (SC, D) remodelled their rhizosphere via storage structures to sustain rapid above-ground growth (Jacoby & Kopriva, 2019). Conversely, low-plasticity species (XH, TY) maintained a stable rhizochemical profile, reducing reliance on metabolic restructuring (Wiesenbauer et al., 2025). This plasticity-linked strategy divergence is an adaptive trade-off for unpredictable stress (He et al., 2024). The significant negative correlation between metabolic plasticity and root: shoot ratio change provided quantitative support for this trade-off.

Consistent down-regulation of AMP, Gluconate, Glutamine and L-Glutamic-acid across most species reflected a shared flowering resource-mobilization mechanism. Notably, reduced Glutamine and L-Glutamic-acid indicated targeted nitrogen flux reallocation to above-ground reproductive tissues (Yoo et al., 2020). Simultaneously, species-specific metabolic signatures emerged: L-citrulline (accumulated in D) may enhance reproductive drought tolerance (Ahmadi et al., 2020); L-leucine (enriched in MN, TY) supports rapid shoot protein synthesis during flowering (Ren et al., 2025). These patterns demonstrated desert ephemerals have evolved conserved core responses and species-specific specialization within shared developmental programmes.

### 4.2 | Rhizosphere bacterial community succession

Unlike most studies focusing on the biogeography of plant–microbe interactions that assumed abiotic filters as the primary driver of microbial community changes, our study confirmed that in water-limited ecosystems, host genetics and developmental status were

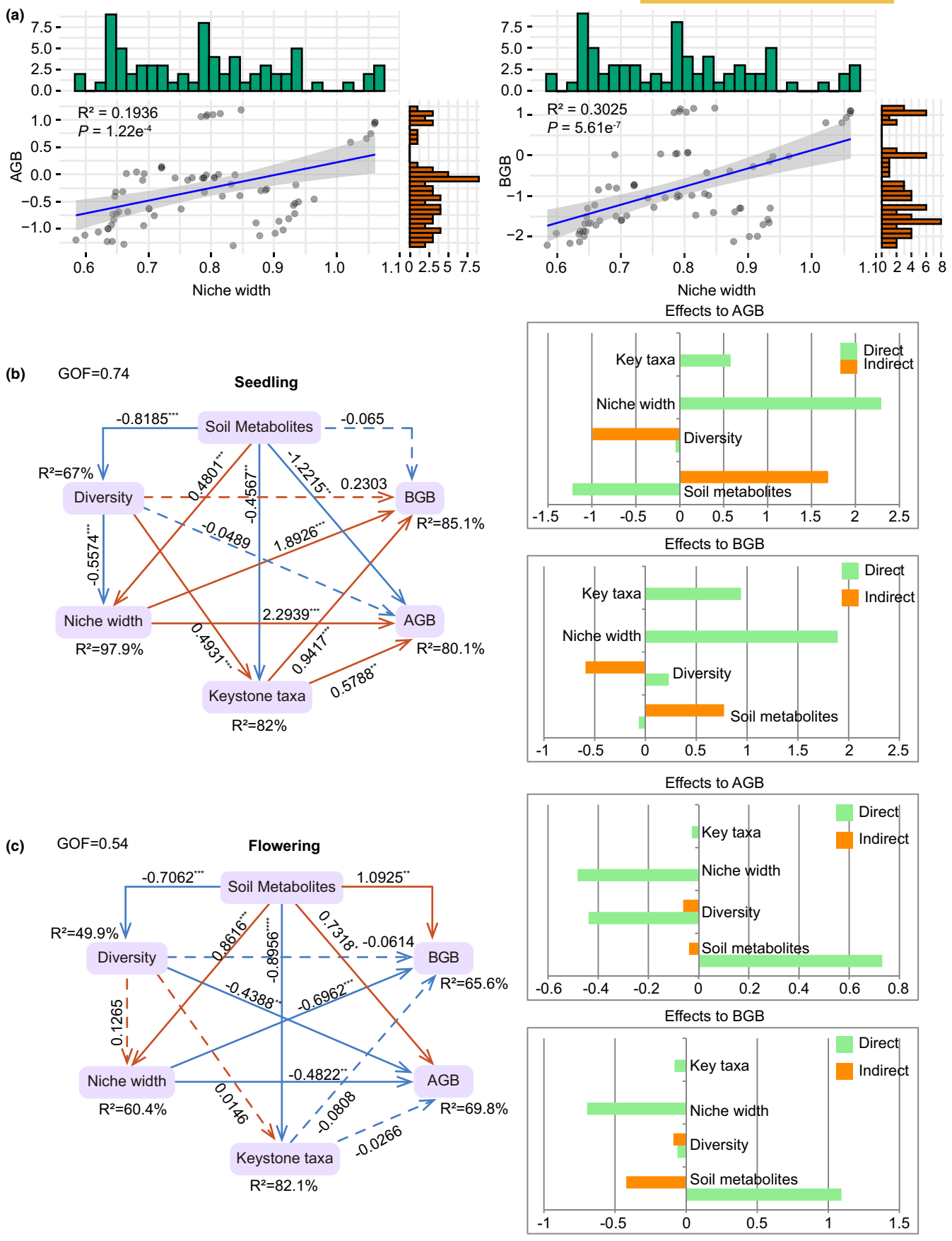



FIGURE 9 (a) Correlation between rhizobacterial niche width and desert ephemeral plant biomass. (b, c) Partial least squares path modelling (PLS-PM) illustrating relationships between soil metabolites, rhizobacterial α-diversity, niche width, keystone taxa and plant biomass. Arrow labels = path coefficients (red/blue = positive/negative effects; solid/dashed arrows = significant/non-significant paths). ***$p < 0.001$, **$p < 0.01$, *$p < 0.05$. $R^2$ denotes the proportion of variance explained for each dependent variable.

the key regulators, with abiotic filters playing only a secondary role (Figure 3). This discrepancy may have resulted from the study being conducted at only one site; within a local small region, environmental heterogeneity (e.g. soil properties, climate) was low, so the results did not replicate those of large-scale studies (Xiong et al., 2021). Such development-dependent succession reflected adaptive plant–microbe tuning to desert environments (Wang, Crabbe, et al., 2025). Divergent niche-width dynamics (TY/XH expansion; D/SC contraction) corresponded with species-specific metabolic strategies, indicating coordinated above-ground–below-ground specialization (Peng et al., 2025; Wang, Xia, et al., 2025).

FAPROTAX revealed a distinct developmental predicted functional shift (Figure 5). Carbon mineralization at the seedling stage supported root establishment (Talbot & Monfet, 2024). Increased nitrogen fixation at flowering met reproductive nitrogen demand (Yoshida et al., 2025) and enhanced drought resistance (Lopez et al., 2023). Notably, only D had an opposite trajectory, likely driven by high metabolic plasticity and fleshy taproot. Labile carbon and nitrogen sources declined, while decomposing roots released complex carbon (Pate et al., 1990), forming a recalcitrant carbon environment. This favoured complex carbon degradation (Zhalnina et al., 2018) and caused a shift towards carbon mining rather than convergent nitrogen acquisition.

Key functions were regulated by development and host phylogeny. Overall, functions converged from seedling carbon transformation to flowering nitrogen cycling and stress tolerance, with decomposers (Molina-Menor et al., 2020) and drought-tolerant nitrogen-taxa (González-Cortés et al., 2022; Tang et al., 2020) dominating respective stages. However, these convergent functions were achieved by distinct microbial taxa across species. D shifted function from decomposition to carbon mineralization and stress tolerance. SC transitioned from energy regulation to nitrogen transformation. DF exhibited highly specialized functions at flowering. MN recruited oligotrophic taxa to cope with environmental fluctuations (Fierer, 2017). TY enlisted *Streptomyces* to enhance chemical competition (Essarioui et al., 2017). XH assembled multifunctional taxa to improve stress tolerance (Singh et al., 2023). These reflect lineage-specific microbiome strategies (Graham et al., 2025). The absence of shared keystone taxa enabled distinct microbial recruitment, reduced niche overlap and facilitated species coexistence (Marasco et al., 2022). Rhizosphere assembly depended on host phylogeny and stage-specific demands rather than a universal core microbiome (Poorter et al., 2012), with functional convergence as an evolutionary innovation (Shelake et al., 2026).

Rhizobacterial succession (seedling–flowering) displayed simpler networks, more positive interactions and lower α-diversity (Figures 4 and 6), reflecting a competitive-to-cooperative shift under harsh arid conditions (Wang et al., 2024). High niche overlap in such environments promoted cooperation among functionally redundant microbes to share limited resources (Portal-Gonzalez et al., 2025). SC and MN exhibited greater network complexity at flowering, associated with high metabolic plasticity to support rapid above-ground growth. Such exceptions indicated network simplification is a general adaptive strategy modulated by host traits, highlighting context-dependent assembly rules (Bittleston et al., 2020).

### 4.3 | Dynamic restructuring of rhizobacteria-metabolite interactions during plant development

This study showed desert ephemerals' rhizobacteria-metabolite network was strongly restructured across development, shifting from broad to targeted microbial recruitment (Figure 8; Fan et al., 2025). Dense seedling correlations reflected an exploratory mode, where root metabolites rapidly assemble microbiomes for nutrient acquisition (Zhang, Ruan, et al., 2024). The sharp decline in correlations at flowering indicated plants redirected resources to reproduction, recruiting nitrogen-fixing and stress-tolerant microbes via targeted signalling to meet reproductive nitrogen demand and stress resistance (Han et al., 2023), supporting an establishment-to-reproduction resource allocation strategy.

However, network restructuring was phylogenetically constrained, not uniform. Network contraction in D, DF and XH aligned with conservative or specialized strategies, while expansion in SC and TY reflected elevated reproductive and competitive demands. MN maintained network stability, matching its balanced adaptation to shallow rooted and fluctuating habitats. These divergent chemical crosstalk patterns correspond to distinct allocation priorities (Zhalnina et al., 2018), driving functional convergence, reducing niche overlap to facilitate coexistence via phylogenetically constrained plant–microbe interactions (Karimi et al., 2021).

These genotype-dependent network patterns were further exemplified by species-specific microbial–metabolite regulatory trajectories. In D, nitrogen-fixing and drought-tolerant taxa supported seedling-stage nitrogen metabolism and stress resistance (Maurice et al., 2024; Zhao et al., 2025), while flowering-stage dominance of iron-reducing *Ferrovibrio* enhanced iron bioavailability for reproduction (Liu, Wang, et al., 2025). DF adopted a streamlined efficiency strategy via low metabolic plasticity, forming specialized associations with *Agromyces* and *Segetibacter* for L-Glutamic-acid utilization (Kim et al., 2021). XH relied on low plasticity but high microbial dependency: *TM7a* facilitated seedling-stage nitrogen and carbon reserve accumulation (e.g. Glutamine, Trehalose-6-phosphate; Zhang, Liu, et al., 2024), while flowering-stage *Nakamurella* regulated nitrogen metabolites and enhanced arsenic detoxification (Li et al., 2024). SC's high metabolic plasticity enabled dynamic rhizosphere remodelling: *Edaphobaculum* supported seedling energy mobilization (Liu, Li, et al., 2025), whereas flowering-stage *Nocardioides* and *Pseudorhodoplanes* drove nitrogen turnover for reproduction (Wang, Chen, et al., 2025). Despite convergent developmental restructuring in MN and TY, their regulatory architectures remained genotype-specific, indicating divergent microbial pathways for conserved ecological functions, with such holobiont reconfiguration underpinning desert species coexistence (Portal-Gonzalez et al., 2025).

### 4.4 | Bacterially mediated feedback on plant performance: A stage-dependent interaction

Rhizosphere microbe–metabolite restructuring underpins a stage-dependent microbial feedback on plant performance. PLS-PM analysis showed that rhizobacterial diversity significantly negatively affected niche width at the seedling stage (Figure 9). This means elevated diversity in resource-poor desert soils intensifies carbon sources and nutrients competition, offsetting diversity advantages via 'competition-induced niche compression' and making niche width the core seedling establishment driver (Marasco et al., 2022; Newberger et al., 2025). A broad niche sustains diverse nutrient cycling for redundancy (Feng et al., 2020), thereby robustly supporting root establishment (Manriquez et al., 2021). Concurrently, keystone taxa enhanced biomass accumulation by mobilizing organic matter nutrients (Wang, Luo, et al., 2025). At this stage, soil metabolites exerted a negative effect on biomass, likely as they were mostly consumed as microbial attractants, forming a metabolites-microbes-biomass indirect support chain (Sasse et al., 2018).

However, this relationship reversed at flowering, reflecting a strategic shift from 'establishment-priority' to 'reproduction-priority'. The community shifted towards specialization and low diversity, narrowing the niche width (Diaz-Gonzalez et al., 2025). This reduced microbial carbon competition, decoupled plant–microbe dependence and enabled independent carbon allocation. It aligned with ecological economic theory that assimilates shift from microbes to reproductive sinks (Castorena et al., 2022). Meanwhile, weakened diversity effects on niche width reduced microbial competition, with remaining microbiota focusing on predicted nitrogen cycling-related functions (Wicaksono et al., 2024). Rhizosphere metabolites shifted from microbial carbon consumption indicators to direct reproductive support (Sasse et al., 2018), dominating flowering-stage biomass accumulation. PLS-PM explanatory power changes confirmed a system-wide driver shift. This transition quantifies 'plant–microbe–metabolite' adaptive coordination under extreme resources, supporting desert ephemerals' stage-specific growth–reproduction balance.

In conclusion, host developmental stages orchestrate a fundamental shift in above-ground–below-ground strategies within the constrained lifespan of desert ephemerals. While the specific rhizobacterial and molecular constituents are species-specific, a convergent suite of successional patterns emerges across species: biomass prioritization shifts to above-ground, rhizosphere metabolic space contracts, bacterial networks simplify and microbiome functions pivot from carbon to nitrogen metabolism. Crucially, path analysis reveals that the driver of plant biomass undergoes a stage-dependent reversal: from reliance on a broad bacterial niche for below-ground establishment to direct dependence on rhizosphere metabolites for above-ground reproduction. This strategic transition from microbially assisted establishment to metabolite-driven reproduction represents a unifying ecological mechanism for optimizing fitness under extreme resource limitation.

## AUTHOR CONTRIBUTIONS

Yang Yang and Weiguo Liu collaboratively designed and discussed the conceptual idea. Yang Yang and Weiguo Liu actively conducted the field sampling and collected the data. Yang Yang performed data curation and analysis. Yang Yang was involved in the creation of the original draft. Weiguo Liu, Xiaodong Yang, Xi-En Long and Yangyang Jia reviewed and edited the manuscript. All authors contributed critically to the drafts and gave final approval for publication.

## ACKNOWLEDGEMENTS

This study was financially supported by the National Natural Science Foundation of China (grant nos.: 32160281 and 32460321) and the Key Laboratory Project, Xinjiang (grant no. 2021D0400).

## CONFLICT OF INTEREST STATEMENT

The author has nothing to declare.

## DATA AVAILABILITY STATEMENT

Data are available from the Dryad Digital Repository: https://doi.org/10.5061/dryad.7d7wm389d (Yang et al., 2026).

## ORCID

*Weiguo Liu* https://orcid.org/0000-0002-6284-9881
*Xiaodong Yang* https://orcid.org/0000-0002-3553-2125

## REFERENCES

Ahmadi, H., Babalar, M., Sarcheshmeh, M. A. A., Morshedloo, M. R., & Shokrpour, M. (2020). Effects of exogenous application of citrulline on prolonged water stress damages in hyssop (*Hyssopus officinalis* L.): Antioxidant activity, biochemical indices, and essential oils profile. *Food Chemistry*, *333*, 127433. https://doi.org/10.1016/j.foodchem.2020.127433

Araya, J. P., Gonzalez, M., Cardinale, M., Schnell, S., & Stoll, A. (2019). Microbiome dynamics associated with the Atacama Flowering Desert. *Frontiers in Microbiology*, *10*, 3160. https://doi.org/10.3389/fmicb.2019.03160

Bao, S. D. (2000). *Soil and agricultural chemistry analysis*.

Bittleston, L. S., Gralka, M., Leventhal, G. E., Mizrahi, I., & Cordero, O. X. (2020). Context-dependent dynamics lead to the assembly of functionally distinct microbial communities. *Nature Communications*, *11*, 1440. https://doi.org/10.1038/s41467-020-15169-0

Caporaso, J. G., Lauber, C. L., Walters, W. A., Berg-Lyons, D., Lozupone, C. A., Turnbaugh, P. J., Fierer, N., & Knight, R. (2011). Global patterns of 16S rRNA diversity at a depth of millions of sequences per sample. *Proceedings of the National Academy of Sciences of the United States of America*, *108*(Suppl 1), 4516–4522. https://doi.org/10.1073/pnas.1000080107

Castorena, M., Olson, M. E., Enquist, B. J., & Fajardo, A. (2022). Toward a general theory of plant carbon economics. *Trends in Ecology & Evolution*, *37*, 829–837. https://doi.org/10.1016/j.tree.2022.05.007

Chen, Y. F., Zhang, L. W., Shi, X., Liu, H. L., & Zhang, D. Y. (2019). Life history responses of two ephemeral plant species to increased precipitation and nitrogen in the Gurbantunggut Desert. *PeerJ*, *7*, e6158. https://doi.org/10.7717/peerj.6158

Chen, Z. C., Shi, Z. Y., Tian, C. Y., & Feng, G. (2008). Effects of arbuscular mycorrhizal fungal inoculation on growth and nutrient uptake of two ephemeral plants. *Chinese Journal of Plant Ecology*, *32*, 6. (in Chinese). https://doi.org/10.3773/j.issn.1005-264x.2008.03.014

Diaz-Gonzalez, S., Gonzalez-Bodi, S., Gonzalez-Sanz, C., Marin, P., Brunner, F., & Sacristan, S. (2025). Maize associated bacterial and fungal microbiomes show contrasting conformation patterns dependent on plant compartment and water availability. *BMC Plant Biology*, *25*, 448. https://doi.org/10.1186/s12870-025-06465-2

Ding, R., Nobrega, R. L. B., & Prentice, I. C. (2025). Global assessment of environmental and plant-trait influences on root: Shoot biomass ratios. *Global Change Biology*, *31*, e70543. https://doi.org/10.1111/gcb.70543

Edwards, J., Johnson, C., Santos-Medellin, C., Lurie, E., Podishetty, N. K., Bhatnagar, S., Eisen, J. A., & Sundaresan, V. (2015). Structure, variation, and assembly of the root-associated microbiomes of rice. *Proceedings of the National Academy of Sciences of the United States of America*, *112*, E911–E920. https://doi.org/10.1073/pnas.1414592112

Essarioui, A., LeBlanc, N., Kistler, H. C., & Kinkel, L. L. (2017). Plant community richness mediates inhibitory interactions and resource competition between streptomyces and fusarium populations in the rhizosphere. *Microbial Ecology*, *74*, 157–167. https://doi.org/10.1007/s00248-016-0907-5

Fan, L. L., Li, Y. M., Ma, J., Mao, J. F., & Wang, L. (2022). Snow and rainfall independently affect the density, composition and productivity of ephemerals in a temperate desert. *Science of the Total Environment*, *807*, 151033. https://doi.org/10.1016/j.scitotenv.2021.151033

Fan, X. Y., Ge, A. H., Qi, S. S., Guan, Y. F., Wang, R., Yu, N., & Wang, E. (2025). Root exudates and microbial metabolites: Signals and nutrients in plant-microbe interactions. *Science China Life Sciences*, *68*, 2290–2302. https://doi.org/10.1007/s11427-024-2876-0

Feng, K., Wang, S., Wei, Z., Wang, Z., Zhang, Z., Wu, Y., Zhang, Y., & Deng, Y. (2020). Niche width of above- and below-ground organisms varied in predicting biodiversity profiling along a latitudinal gradient. *Molecular Ecology*, *29*, 1890–1902. https://doi.org/10.1111/mec.15441

Fierer, N. (2017). Embracing the unknown: Disentangling the complexities of the soil microbiome. *Nature Reviews Microbiology*, *15*, 579–590. https://doi.org/10.1038/nrmicro.2017.87

Funk, J. L., Larson, J. E., Blair, M. D., Nguyen, M. A., & Rivera, B. (2024). Drought response in herbaceous plants: A test of the integrated framework of plant form and function. *Functional Ecology*, *38*, 679–691. https://doi.org/10.1111/1365-2435.14495

González-Cortés, J. J., Valle, A., Ramírez, M., & Cantero, D. (2022). Characterization of bacterial and archaeal communities by DGGE and next generation sequencing (NGS) of nitrification bioreactors using two different intermediate landfill leachates as ammonium substrate. *Waste and Biomass Valorization*, *13*, 3753–3766. https://doi.org/10.1007/s12649-022-01759-0

Graham, N. J., Day, N. J., Slavov, G., Ritchie, P., & Wakelin, S. A. (2025). Evidence of Phylosymbiosis in the microbiome of conifer roots. *Phytobiomes Journal*, *9*, 541–557. https://doi.org/10.1094/pbiomes-03-25-0022-r

Hacquard, S., & Martin, F. M. (2024). The chemical language of plant-microbe-microbe associations: An introduction to a virtual issue. *New Phytologist*, *244*, 739–742. https://doi.org/10.1111/nph.20124

Han, M. G., Chen, Y., Sun, L. J., Yu, M., Li, R., Li, S. F., Su, J. R., & Zhu, B. (2023). Linking rhizosphere soil microbial activity and plant resource acquisition strategy. *Journal of Ecology*, *111*, 875–888. https://doi.org/10.1111/1365-2745.14067

He, C., Jin, M., Liu, W., Shan, L. S., Li, Y., Zhang, Z. Z., Li, Q., Li, M., Jin, N., & Hu, F. (2024). The metabolomics and transcriptomics of reveal age-related molecular alterations under naturally high temperature and drought conditions. *Physiologia Plantarum*, *176*, e14129. https://doi.org/10.1111/ppl.14129

Hemelda, N. M., & Noutoshi, Y. (2025). Root-exuded sugars as drivers of rhizosphere microbiome assembly. *Plant Biotechnology*, *42*, 215–227. https://doi.org/10.5511/plantbiotechnology.25.0214a

Huang, G., Li, Y., & Padilla, F. M. (2015). Ephemeral plants mediate responses of ecosystem carbon exchange to increased precipitation in a temperate desert. *Agricultural and Forest Meteorology*, *201*, 141–152. https://doi.org/10.1016/j.agrformet.2014.11.011

Jacoby, R. P., & Kopriva, S. (2019). Metabolic niches in the rhizosphere microbiome: New tools and approaches to analyse metabolic mechanisms of plant-microbe nutrient exchange. *Journal of Experimental Botany*, *70*, 1087–1094. https://doi.org/10.1093/jxb/ery438

Jiang, M., Delgado-Baquerizo, M., Yuan, M. M., Ding, J., Yergeau, E., Zhou, J., Crowther, T. W., & Liang, Y. (2023). Home-based microbial solution to boost crop growth in low-fertility soil. *New Phytologist*, *239*, 752–765. https://doi.org/10.1111/nph.18943

Karimi, N., Larkin, D. J., Glasenhardt, M.-C., Barak, R. S., Williams, E. W., Ernst, A. R., & Hipp, A. L. (2021). Selection on convergent functional traits drives compositional divergence in early succession of a tallgrass prairie restoration experiment. *Journal of Ecology*, *110*, 415–429. https://doi.org/10.1111/1365-2745.13808

Kim, D. R., Jeon, C. W., Cho, G., Thomashow, L. S., Weller, D. M., Paik, M. J., Lee, Y. B., & Kwak, Y. S. (2021). Glutamic acid reshapes the plant microbiota to protect plants against pathogens. *Microbiome*, *9*, 244. https://doi.org/10.1186/s40168-021-01186-8

Knight, R., Vrbanac, A., Taylor, B. C., Aksenov, A., Callewaert, C., Debelius, J., Gonzalez, A., Kosciolek, T., McCall, L. I., McDonald, D., Melnik, A. V., Morton, J. T., Navas, J., Quinn, R. A., Sanders, J. G., Swafford, A. D., Thompson, L. R., Tripathi, A., Xu, Z. Z., … Dorrestein, P. C. (2018). Best practices for analysing microbiomes. *Nature Reviews Microbiology*, *16*, 410–422. https://doi.org/10.1038/s41579-018-0029-9

Kozich, J. J., Westcott, S. L., Baxter, N. T., Highlander, S. K., & Schloss, P. D. (2013). Development of a dual-index sequencing strategy and curation pipeline for analyzing amplicon sequence data on the MiSeq Illumina sequencing platform. *Applied and Environmental Microbiology*, *79*, 5112–5120. https://doi.org/10.1128/AEM.01043-13

Lei, Z., Zhang, H., Liu, W., Sheng, J., Zhang, H., Wang, Y., Tang, Y., Wang, H., Ding, C., Qiao, W., Zhu, Y., Yang, G., Zhang, Y., Liu, Z., Zhou, N., Hu, C., & Zhao, X. (2025). Dynamic and stable core microbiota assist plants in enriching selenium and reducing cadmium absorption. *Advanced Science*, *12*, e00862. https://doi.org/10.1002/advs.202500862

Li, G. L., Zhang, D. H., Zhang, Z. S., Hu, Y. G., Huang, L., & Lu, L. N. (2021). Population dynamics of main sand-fixing shrubs in the Gurbantunggut Desert. *Journal of Desert Research*, *41*, 129–137. (in Chinese). https://doi.org/10.7522/j.issn.1000-694X.2020.00103

Li, J. Y., Zhu, Z., Lv, X. L., Hu, X., Tan, H. X., Liu, W. C., & Luo, G. Z. (2024). Exploring single-stage oxic process for simultaneous rapid recovery of phosphate and nitrate via bioflocs to promote circular economic. *Chemical Engineering Journal*, *497*, 154575. https://doi.org/10.1016/j.cej.2024.154575

Liu, C., Mansoldo, F. R. P., Li, H., Vermelho, A. B., Zeng, R. J., Li, X., & Yao, M. (2025). A workflow for statistical analysis and visualization of microbiome omics data using the R microeco package. *Nature Protocols*, *21*, 1300–1324. https://doi.org/10.1038/s41596-025-01239-4

Liu, W. Y., Wang, G. Q., Wen, S. M., Zhao, Y. W., Ding, Y. X., Yao, B. H., Wang, Z. L., Shu, D. T., Wei, G. H., Chen, J., & Shangguan, Z. P. (2025). Microbiome-mediated mechanisms regulating adaptability to iron deficiency in the intercropping system of soybean and maize. *Agronomy*, *15*, 286. https://doi.org/10.3390/agronomy15020286

Liu, Y., Li, B., Chen, T., Tian, S., & Zhang, Z. (2025). The synthesis, degradation and biological function of trehalose- 6-phosphate. *Stress Biology*, *5*, 38. https://doi.org/10.1007/s44154-025-00235-8

Lopez, C. M., Alseekh, S., Torralbo, F., Martinez Rivas, F. J., Fernie, A. R., Amil-Ruiz, F., & Alamillo, J. M. (2023). Transcriptomic and metabolomic analysis reveals that symbiotic nitrogen fixation enhances

drought resistance in common bean. *Journal of Experimental Botany*, *74*, 3203–3219. https://doi.org/10.1093/jxb/erad083

Louca, S., Parfrey, L. W., & Doebeli, M. (2016). Decoupling function and taxonomy in the global ocean microbiome. *Science*, *353*, 1272–1277. https://doi.org/10.1126/science.aaf4507

Manriquez, B., Muller, D., & Prigent-Combaret, C. (2021). Experimental evolution in plant-microbe systems: A tool for deciphering the functioning and evolution of plant-associated microbial communities. *Frontiers in Microbiology*, *12*, 619122. https://doi.org/10.3389/fmicb.2021.619122

Marasco, R., Fusi, M., Ramond, J. B., Van Goethem, M. W., Seferji, K., Maggs-Kolling, G., Cowan, D. A., & Daffonchio, D. (2022). The plant rhizosheath-root niche is an edaphic "mini-oasis" in hyperarid deserts with enhanced microbial competition. *ISME Communications*, *2*, 47. https://doi.org/10.1038/s43705-022-00130-7

Maurice, K., Laurent-Webb, L., Bourceret, A., Boivin, S., Boukcim, H., Selosse, M. A., & Ducousso, M. (2024). Networking the desert plant microbiome, bacterial and fungal symbionts structure and assortativity in co-occurrence networks. *Environmental Microbiomes*, *19*, 65. https://doi.org/10.1186/s40793-024-00610-4

Molina-Menor, E., Gimeno-Valero, H., Pascual, J., Pereto, J., & Porcar, M. (2020). High culturable bacterial diversity from a European desert: The Tabernas Desert. *Frontiers in Microbiology*, *11*, 583120. https://doi.org/10.3389/fmicb.2020.583120

Neilson, J. W., Quade, J., Ortiz, M., Nelson, W. M., Legatzki, A., Tian, F., LaComb, M., Betancourt, J. L., Wing, R. A., Soderlund, C. A., & Maier, R. M. (2012). Life at the hyperarid margin: Novel bacterial diversity in arid soils of the Atacama Desert, Chile. *Extremophiles*, *16*, 553–566. https://doi.org/10.1007/s00792-012-0454-z

Newberger, D. R., Deel, H. L., Manter, D. K., & Vivanco, J. M. (2025). Effect of intra- and inter-specific plant interactions on the rhizosphere microbiome of a single target plant at different densities. *PLoS One*, *20*, e0316676. https://doi.org/10.1371/journal.pone.0316676

Nour, M. M., Aljabi, H. R., AL-Huqail, A. A., Horneburg, B., Mohammed, A. E., & Alotaibi, M. O. (2024). Drought responses and adaptation in plants differing in life-form. *Frontiers in Ecology and Evolution*, *12*, 1452427. https://doi.org/10.3389/fevo.2024.1452427

Olesen, J. M., Bascompte, J., Dupont, Y. L., & Jordano, P. (2007). The modularity of pollination networks. *Proceedings of the National Academy of Sciences of the United States of America*, *104*, 19891–19896. https://doi.org/10.1073/pnas.0706375104

Pacheco-Moreno, A., Bollmann-Giolai, A., Chandra, G., Brett, P., Davies, J., Thornton, O., Poole, P., Ramachandran, V., Brown, J. K. M., Nicholson, P., Ridout, C., DeVos, S., & Malone, J. G. (2024). The genotype of barley cultivars influences multiple aspects of their associated microbiota via differential root exudate secretion. *PLoS Biology*, *22*, e3002232. https://doi.org/10.1371/journal.pbio.3002232

Pate, J. S., Froend, R. H., Bowen, B. J., Hansen, A., & Kuo, J. (1990). Seedling growth and storage characteristics of seeder and Resprouter species of Mediterranean-type ecosystems of S. W. Australia. *Annals of Botany*, *65*, 585–601. https://doi.org/10.1093/oxfordjournals.aob.a087976

Peng, Y., Fornara, D. A., Yue, K., Peng, X., Peng, C. H., Wu, Q. Q., Ni, X. Y., Liao, S., Yang, Y. S., Wu, F. Z., & Peñuelas, J. (2022). Globally limited individual and combined effects of multiple global change factors on allometric biomass partitioning. *Global Ecology and Biogeography*, *31*, 454–469. https://doi.org/10.1111/geb.13438

Peng, Z., Zhang, Y., Li, X., Gao, H., Liu, Y., An, Y., Qian, X., Wei, G., & Jiao, S. (2025). Trait-based life history strategies shape bacterial niche breadth. *Advanced Science*, *12*, e2405947. https://doi.org/10.1002/advs.202405947

Poorter, H., Niklas, K. J., Reich, P. B., Oleksyn, J., Poot, P., & Mommer, L. (2012). Biomass allocation to leaves, stems and roots: Meta-analyses of interspecific variation and environmental control. *New Phytologist*, *193*, 30–50. https://doi.org/10.1111/j.1469-8137.2011.03952.x

Portal-Gonzalez, N., Wang, W., He, W., & Santos-Bermudez, R. (2025). Engineering plant holobionts for climate-resilient agriculture. *The ISME Journal*, *19*, wraf158. https://doi.org/10.1093/ismejo/wraf158

Puglielli, G., Laanisto, L., Poorter, H., & Niinemets, U. (2021). Global patterns of biomass allocation in woody species with different tolerances of shade and drought: Evidence for multiple strategies. *New Phytologist*, *229*, 308–322. https://doi.org/10.1111/nph.16879

Quast, C., Pruesse, E., Yilmaz, P., Gerken, J., Schweer, T., Yarza, P., Peplies, J., & Glockner, F. O. (2013). The SILVA ribosomal RNA gene database project: Improved data processing and web-based tools. *Nucleic Acids Research*, *41*, D590–D596. https://doi.org/10.1093/nar/gks1219

Ren, X., Huang, Y., Zhang, L., Lu, Q., Wang, X., Ying, W., & Ruan, S. (2025). Integrated analysis of transcriptomics and metabolomics of Dendrobium officinale flowers at different developmental stages. *Scientific Reports*, *15*, 10342. https://doi.org/10.1038/s41598-025-93889-3

Sasse, J., Martinoia, E., & Northen, T. (2018). Feed your friends: Do plant exudates shape the root microbiome? *Trends in Plant Science*, *23*, 25–41. https://doi.org/10.1016/j.tplants.2017.09.003

She, W., Bai, Y., Zhang, Y., Qin, S., Liu, Z., & Wu, B. (2017). Plasticity in meristem allocation as an adaptive strategy of a desert shrub under contrasting environments. *Frontiers in Plant Science*, *8*, 1933. https://doi.org/10.3389/fpls.2017.01933

Shelake, R. M., Waghunde, R. R., & Kim, J. Y. (2026). Coevolution of plant-microbe interactions, friend-foe continuum, and microbiome engineering for a sustainable future. *Molecular Plant*, *19*, 719–754. https://doi.org/10.1016/j.molp.2026.01.010

Singh, A., Mazahar, S., Chapadgaonkar, S. S., Giri, P., & Shourie, A. (2023). Phyto-microbiome to mitigate abiotic stress in crop plants. *Frontiers in Microbiology*, *14*, 1210890. https://doi.org/10.3389/fmicb.2023.1210890

Talbot, M. H., & Monfet, D. (2024). Development of a crop growth model for the energy analysis of controlled agriculture environment spaces. *Biosystems Engineering*, *238*, 38–50. https://doi.org/10.1016/j.biosystemseng.2023.12.012

Tang, X., Xie, G., Shao, K., Hu, Y., Cai, J., Bai, C., Gong, Y., & Gao, G. (2020). Contrast diversity patterns and processes of microbial community assembly in a river-lake continuum across a catchment scale in northwestern China. *Environmental Microbiomes*, *15*, 10. https://doi.org/10.1186/s40793-020-00356-9

Wang, J., Shi, X., Tan, Y., Wang, L., & Zhang, G. (2023). Elevated $O_3$ exerts stronger effects than elevated $CO_2$ on the functional guilds of fungi, but collectively increase the structural complexity of fungi in a paddy soil. *Microbial Ecology*, *86*, 1096–1106. https://doi.org/10.1007/s00248-022-02124-3

Wang, M., Ge, A. H., Ma, X., Wang, X., Xie, Q., Wang, L., Song, X., Jiang, M., Yang, W., Murray, J. D., Wang, Y., Liu, H., Cao, X., & Wang, E. (2024). Dynamic root microbiome sustains soybean productivity under unbalanced fertilization. *Nature Communications*, *15*, 1668. https://doi.org/10.1038/s41467-024-45925-5

Wang, R., Chen, Y., Zhang, H., Wang, Z., Zheng, F., Mu, Y., Bao, H., Ma, Z., Chu, C., & Yang, Y. (2025). Plant–microbe interactions drive the rhizosphere microbial assembly and nitrogen cycling in a subtropical forest. *Functional Ecology*, *39*, 1274–1287. https://doi.org/10.1111/1365-2435.70025

Wang, W., Xia, Y., Zhang, P., Zhu, M., Huang, S., Sun, X., Xu, Z., Zhang, N., Xun, W., Shen, Q., Miao, Y., & Zhang, R. (2025). Narrow-spectrum resource-utilizing bacteria drive the stability of synthetic communities through enhancing metabolic interactions. *Nature Communications*, *16*, 6088. https://doi.org/10.1038/s41467-025-61432-7

Wang, Y., Luo, X., Yue, M., Song, B., Karhu, K., & Razavi, B. S. (2025). Rhizosphere keystone microbiomes promote invasive plant growth

under PLA and PVC microplastic stress: A comparative study with native species. *Environmental Science & Technology*, *59*, 20201–20215. https://doi.org/10.1021/acs.est.5c06285

Wang, Z. Y., Crabbe, M. J. C., Zhang, Y. Q., & Liu, B. R. (2025). Fertile Island effects across developmental stages of nebkhas drive microbial nutrient cycling in arid ecosystems. *Catena*, *259*, 109373. https://doi.org/10.1016/j.catena.2025.109373

Wen, T., Niu, G., Chen, T., Shen, Q., Yuan, J., & Liu, Y. X. (2023). The best practice for microbiome analysis using R. *Protein & Cell*, *14*, 713–725. https://doi.org/10.1093/procel/pwad024

Wicaksono, W. A., Köberl, M., White, R. A., Jansson, J. K., Jansson, C., Cernava, T., & Berg, G. (2024). Plant-specific microbial diversity facilitates functional redundancy at the soil-root interface. *Plant and Soil*. https://doi.org/10.1007/s11104-024-07097-5

Wiesenbauer, J., Gorka, S., Jenab, K., Schuster, R., Kumar, N., Rottensteiner, C., König, A., Kraemer, S., Inselsbacher, E., & Kaiser, C. (2025). Preferential use of organic acids over sugars by soil microbes in simulated root exudation. *Soil Biology and Biochemistry*, *203*, 109738. https://doi.org/10.1016/j.soilbio.2025.109738

Wilson, B., & Hayek, L. A. C. (2015). Distinguishing relative specialist and generalist species in the fossil record. *Marine Micropaleontology*, *119*, 7–16. https://doi.org/10.1016/j.marmicro.2015.07.001

Xiong, C., Singh, B. K., He, J. Z., Han, Y. L., Li, P. P., Wan, L. H., Meng, G. Z., Liu, S. Y., Wang, J. T., Wu, C. F., Ge, A. H., & Zhang, L. M. (2021). Plant developmental stage drives the differentiation in ecological role of the maize microbiome. *Microbiome*, *9*, 171. https://doi.org/10.1186/s40168-021-01118-6

Yang, G., Liu, W., Mo, X., & Mei, Z. (2025). Alpine adaptive mechanism on rhizosphere microbes recruitment of *Crepis napifera* (Franch.) Babc. by multi-omics analysis. *Biology*, *14*, 345. https://doi.org/10.3390/biology14040345

Yang, Y., Liu, W. G., Long, X.-E., Jia, Y. Y., & Yang, X. D. (2026). Data from: Linking rhizosphere bacterial succession to metabolite dynamics unravels the underlying survival strategies of desert ephemeral plants [dataset]. *Dryad*. https://doi.org/10.5061/dryad.7d7wm389d

Yoo, H. C., Yu, Y. C., Sung, Y., & Han, J. M. (2020). Glutamine reliance in cell metabolism. *Experimental & Molecular Medicine*, *52*, 1496–1516. https://doi.org/10.1038/s12276-020-00504-8

Yoshida, H., Itoh, H., Mori, M., Koketsu, E., Kawamura, M., Nishio, S., Mori, H., & Matsuoka, M. (2025). Photoperiodic flowering regulators are required for nitrogen-dependent flowering delay in rice under long-day condition. *Nature Communications*, *16*, 9231. https://doi.org/10.1038/s41467-025-64299-w

Zeng, Y., Liu, T., Zhou, X. B., Sun, Q. M., Han, Z. Q., & Liu, K. (2016). Effects of climate change on plant composition and diversity in the Gurbantünggüt Desert of northwestern China. *Ecological Research*, *31*, 427–439. https://doi.org/10.1007/s11284-016-1352-0

Zhalnina, K., Louie, K. B., Hao, Z., Mansoori, N., da Rocha, U. N., Shi, S., Cho, H., Karaoz, U., Loque, D., Bowen, B. P., Firestone, M. K., Northen, T. R., & Brodie, E. L. (2018). Dynamic root exudate chemistry and microbial substrate preferences drive patterns in rhizosphere microbial community assembly. *Nature Microbiology*, *3*, 470–480. https://doi.org/10.1038/s41564-018-0129-3

Zhang, H., Ruan, Y., Kuzyakov, Y., Qiao, Y. Z., Xu, Q. C., Huang, Q. W., Shen, Q. R., & Ling, N. (2024). Carbon flow from roots to rhizobacterial networks: Grafting effects. *Soil Biology and Biochemistry*, *199*, 109580. https://doi.org/10.1016/j.soilbio.2024.109580

Zhang, M., Liu, J. B., Wang, D. B., Lu, M. J., Fan, Y. J., Ji, J. J., & Wu, J. (2024). Combined effects of carbon source and C/N ratio on the partial denitrification performance: Nitrite accumulation, denitrification kinetic and microbial transition. *Journal of Environmental Chemical Engineering*, *12*, 113343. https://doi.org/10.1016/j.jece.2024.113343

Zhang, T., Wang, Z., Lv, X., Dang, H., & Zhuang, L. (2020). Variation of rhizosphere bacterial community diversity in the desert ephemeral plant Ferula sinkiangensis across environmental gradients. *Scientific Reports*, *10*, 18442. https://doi.org/10.1038/s41598-020-75591-8

Zhao, K. F., Zeng, Y., Wang, Y. H., Yang, X. F., Wang, P., Liang, Y. J., & He, J. (2023). Mechanisms for the construction of plant communities in the Gurbantunggut Desert, China. *Ecological Indicators*, *154*, 110615. https://doi.org/10.1016/j.ecolind.2023.110615

Zhao, Q. Y., Cao, X. L., Zhang, L., Hu, X., Zeng, X. J., Wei, Y. M., Zhang, D. B., Xiao, X., Xi, H., & Zhao, S. F. (2025). Analysis of the differences in rhizosphere microbial communities and pathogen adaptability in chili root rot disease between continuous cropping and rotation cropping systems. *Microorganisms*, *13*, 1806. https://doi.org/10.3390/microorganisms13081806

## SUPPORTING INFORMATION

Additional supporting information can be found online in the Supporting Information section at the end of this article.

**Figure S1.** Pictures of seedlings of each ephemeral plant.

**Figure S2.** Pictures of flowerings of each ephemeral plant.

**Figure S3.** Pictures of flowerings of each ephemeral plant.

**Figure S4.** Biomass reallocation patterns and root: shoot ratio changes across desert ephemeral species.

**Figure S5.** Soil physicochemical properties among desert ephemeral plants between seedling and flowering growth periods.

**Figure S6.** Metabolic plasticity correlates with resource allocation.

**Figure S7.** Developmental metabolic dynamics across plant species.

**Figure S8.** Rarefaction analysis of desert ephemeral plants at seedling and flowering periods.

**Figure S9.** Growth stage dynamics of rhizosphere bacterial communities across six plant species.

**Figure S10.** α-diversity of rhizosphere bacteria in the seedling and flowering stages of six ephemeral plants.

**Figure S11.** Rhizosphere bacterial niche width, specialist/generalist proportions, community PCoA and dominant phyla across species and growth stages.

**Figure S12.** Comparison of bacterial phyla between bulk soil and rhizosphere at seedling and flowering stages.

**Figure S13.** Comparison of phyla with significant differences of species D and DF between seedling and flowering periods.

**Figure S14.** Comparison of phyla with significant differences of species MN and SC between seedling and flowering periods.

**Figure S15.** Comparison of phyla with significant differences of species TY and XH between seedling and flowering periods.

**Figure S16.** Species-specific relative abundance of predicted carbon- and nitrogen-related functional groups.

**Figure S17.** Co-occurrence network of rhizosphere bacteria of each ephemeral plant species between the seedling and flowering periods.

**Figure S18.** *Zi-Pi* plot revealing the roles of genera of bacterial community based on their topological properties at the seedling stage.

**Figure S19.** *Zi-Pi* plot revealing the roles of genera of bacterial community based on their topological properties at the flowering stage.

**Figure S20.** Correlation heatmaps of species D keystone taxa–metabolite associations at the seedling and flowering stages.

**Figure S21.** Correlation heatmaps of keystone taxa–metabolite associations for species DF and MN across developmental stages.

**Figure S22.** Correlation heatmaps of keystone taxa–metabolite associations for species SC, TY and XH across developmental stages.
**Table S1.** Key traits of six ephemeral species in the Gurbantünggüt Desert.
**Table S2.** Vegetation coverage and composition at the sampling site.
**Table S3.** Species-level allocation patterns with increased sample sizes.
**Table S4.** Metabolic diversity contraction during plant development.
**Table S5.** PERMANOVA results for full factorial model (Species × Stage).
**Table S6.** Metabolic plasticity metrics and biomass changes by species.
**Table S7.** Metabolites trend among the six plant species based on flowering vs. seedling.
**Table S8.** Consistently changed metabolites based on flowering vs. seedling.
**Table S9.** Marginal effects of explanatory variables on rhizosphere bacterial communities.
**Table S10.** Species environment significance results.
**Table S11.** Generalist and Specialist bacterial taxa in bulk soil and rhizosphere.
**Table S12.** Generalist and Specialist bacterial taxa of each ephemeral plant species during the seedling and flowering periods.
**Table S13.** Pairwise comparison (seedling vs. flowering) of FAPROTAX-predicted functions of each ephemeral plant species.
**Table S14.** Topology characterization of soil bacterial co-occurrence network.
**Table S15.** Comparison of network topological parameters for rhizobacterial communities of different plant species at seedling and flowering stages.
**Table S16.** Importance scores of key bacterial genera linked to specific plant species and growth stages.

**How to cite this article:** Yang, Y., Liu, W., Long, X.-E., Jia, Y., & Yang, X. (2026). Linking rhizosphere bacterial succession to metabolite dynamics unravels the underlying survival strategies of desert ephemeral plants. *Functional Ecology*, *40*, 2083–2101. https://doi.org/10.1111/1365-2435.70374